Photoluminescence and resonant Raman spectra of silicon films produced by size-selected cluster beam deposition

M. Ehbrecht, B. Kohn, and F. Huisken
Max-Planck-Institut für Strömungsforschung, Bunsenstrasse 10, 37073 Göttingen, Germany

M. A. Laguna and V. Paillard
Laboratoire de Physique des Solides, Université Paul Sabatier, 118, Route de Narbonne, 31062 Toulouse Cedex 4, France
(Received 15 April 1997)

Silicon clusters and nanocrystals have been generated by CO_2-laser-induced decomposition of SiH_4 in a flow reactor. By introducing a conical nozzle into the reaction zone, the clusters are extracted into a molecular-beam machine and analyzed with a time-of-flight mass spectrometer (TOFMS). Since the clusters have a size-dependent velocity, a mechanical velocity selector is used to further narrow their size distribution and to select a specific mean size. Employing this technique, silicon clusters with different preselected mean sizes have been deposited at low energy on various substrates. Photoluminescence (PL) and resonant Raman spectra of the resulting films are presented. The crystallite sizes deduced from the Raman spectra confirm the TOFMS measurements. The PL spectra are shifted with decreasing cluster size to smaller wavelengths. Our results agree very well with theoretical predictions for silicon quantum dots. [S0163-1829(97)08035-1]

I. INTRODUCTION

The observation of photoluminescence (PL) from porous nanostructured silicon at the beginning of this decade[1] has triggered an enormous amount of research activity in this field.[2] The motivating force behind this kind of work is the ambition to integrate silicon nanostructures into future optoelectronic devices.[3] The general development towards nanoscaled technology requires a detailed knowledge of the physical and chemical properties of semiconductors in the mesoscopic state of matter. In this regard, silicon clusters and nanocrystals are of particular interest. The structures of small Si_n clusters with $n \leqslant 10$ are well understood,[4] but the transition to the bulk phase, which is realized by nanosized particles, is still the subject of intensive experimental and theoretical work.[5–7]

Two different mechanisms are currently considered to explain photoluminescence in silicon nanostructures. In the quantum confinement model, the photoluminescence is assumed to be due to electron-hole recombination across the fundamental nanostructure band gap.[5] In contrast, the surface state model assumes that surface states act as traps and capture the electron or hole, facilitating their recombination.[8] Most experimental investigations on PL have been performed on porous silicon produced by electrochemical etching of Si wafers,[9,10] but alternative methods of preparation have also been reported, such as plasma-enhanced chemical-vapor deposition (PECVD) from a rf discharge of silane[11] or pyrolysis of disilane.[12] The diameter of the nanostructures is usually determined by transmission electron microscopy and Raman spectroscopy.

At this background, we have employed our recently developed cluster beam source[13–17] for the generation of molecular beams containing silicon clusters and nanoscaled particles. The source is based on the aggregation of CO_2-laser-induced dissociation products in a gas flow reactor. A detailed analysis of the cluster beam, which will be presented in a forthcoming paper, has shown that the velocity of the silicon clusters decreases with increasing mass. Very recently we have demonstrated the possibility of fabricating thin films from silicon clusters, with the mean particle diameter being controlled by combining the cluster beam deposition technique with a velocity selector.[17] The aim of this article is to report results obtained by studying the Raman and photoluminescence spectra of thin films grown from silicon clusters with narrow size distributions around mean particle diameters between 2.5 and 7.0 nm. Since the covalently bonded clusters are deposited at low energy, they neither fragment nor coalesce on the substrate.[18,19] Hence the size distribution of the deposited particles can be determined very precisely prior to the deposition by time-of-flight mass spectrometry.

II. EXPERIMENTAL SETUP

A. Cluster generation and film preparation

The silicon clusters were generated by CO_2-laser-induced decomposition of SiH_4 in a gas flow reactor as has been described in detail elsewhere.[13,14] Figure 1 shows a schematic view of the experimental setup consisting of the cluster beam source and the elements used for deposition. The apparatus contains a laser-driven flow reactor incorporated into the source chamber of a molecular-beam machine and a time-of-flight mass spectrometer (TOFMS), not shown in the figure. The reactant gas, SiH_4, is admitted to the center of the flow reactor through a stainless steel tube of 3 mm diameter. To initiate the decomposition, the gas flow is crossed at right angles with the focused radiation of a line-tunable pulsed CO_2 laser. In order to confine the reactant gas to the flow axis, helium is flushed through a coaxial outer tube with 12 mm diameter. The reaction products are extracted perpendicularly to both the gas flow and the CO_2-laser beam through a conical nozzle with a 0.3-mm-

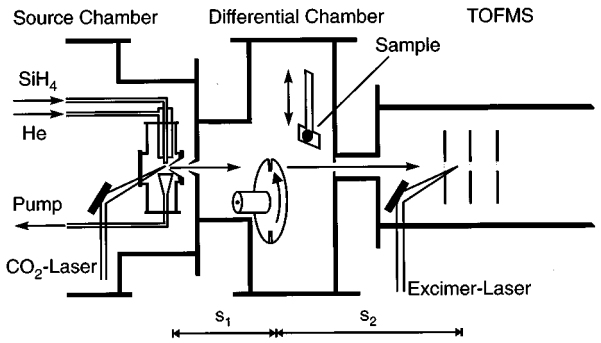

FIG. 1. Schematic view of the cluster generation and deposition setup.

diam opening. In order to achieve a residual pressure of 5×10^{-3} mbar, the source chamber is pumped by a 6000-l/s oil diffusion pump, a 350-m^3/h roots blower, and a 65-m^3/h rotary pump. After skimming, the clusters pass through a pressure-reducing differential chamber of 370 mm length and finally they reach the TOFMS where they are ionized in a Wiley-McLaren-type[20] ion source by the radiation of an ArF excimer laser ($\lambda=193$ nm). In the present experiment, the reactor was operated under the following conditions: 20-sccm (sccm denotes cubic centimeter per minute at STP) flow rate of SiH_4, 1100-sccm flow rate of He, 330-mbar total pressure, 50-mJ CO_2-laser pulse energy on the 10-μP(30) line (934.9 cm^{-1}), focused with a lens 200 mm in focal length.

Since the reaction is driven by a pulsed CO_2 laser the silicon clusters are generated in a pulsed mode. Due to the size-dependent velocity of the extracted particles, the cluster pulse becomes broadened and the clusters are separated according to their size. Thus it is possible to reduce the size distribution of the deposited clusters by introducing a rotating chopper wheel into the cluster beam, as has been demonstrated recently.[17] The disk is 123 mm in diameter and 1 mm thick. It possesses two diametrically opposed 1-mm-wide slits. The chopper is operated at a rotational frequency of 400 Hz, resulting in an opening time of 7.2 μs for a cluster beam of 1 mm width. Using a light barrier, a frequency divider, and a variable delay generator, the CO_2 laser is synchronized with the chopper. The distance s_1 between the nozzle and the chopper disk is 218 mm, while the distance s_2 between the chopper and the ionization region is 321.5 mm. By choosing the appropriate time Δt_1 between the firing of the CO_2 laser and the moment when the particles pass through the chopper, it is possible to select, from the entire cluster pulse, the portion with the desired mean size and to deposit it on the substrate.

Thin films from silicon clusters and nanoparticles can be produced by moving a sample holder, which is located in the differential chamber, into the cluster beam. For the experiments described in this article, room-temperature CaF_2 and LiF substrates were used. Depending on the preselected cluster size, the deposition times were up to 24 h. The background pressure in the deposition chamber, was 5×10^{-5} mbar.

B. Mass spectrometric characterization of the cluster pulse

If the substrate is moved out of the cluster beam, the particles reach the TOFMS, where they are ionized in a Whiley-McLaren-type ion source by the radiation of an ArF-excimer laser. The ion beam is collinear with the neutral cluster beam; so additional ion optics, which must be used in a perpendicular geometry to compensate for the initial kinetic energy, are not necessary. In contrast to earlier experiments[13–17] where a digital scope was used, the time-of-flight mass spectra have been measured by storing the detected ion signals as a function of their arrival time at the detector in a multichannel scaler (EG+G ORTEC, model T914). This device enables measurements at very low ionizing laser fluence since the ion signals can be accumulated over several thousand laser shots. Using the average function of a digital scope, small signals will be lost in the background noise during the averaging process. On the other hand, studies at low laser fluence are necessary to avoid strong fragmentation and/or multiple ionization.

Since the kinetic energy T_0 of large neutral clusters is of the same order of magnitude as the energy T_1 they receive in the ion source, T_0 must not be neglected. Therefore, the relation $t\sim\sqrt{m}$ is not fulfilled anymore. To perform an accurate mass calibration of the time-of-flight (TOF) spectra, the initial velocity of the neutral clusters has to be known. This velocity can be calculated from the distance s_2 and the time Δt_2 the particles need to travel this distance. Then the mass calibration of the TOF spectra can be performed numerically, using the proper geometrical and electrostatical parameters as well as the velocity of the neutral silicon clusters. For example, a peak in the time-of-flight spectrum at $t=400$ μs would correspond to Si^+_{1020} if T_0 is neglected, but to Si^+_{1420} if the measured velocity of $v_0=1500$ m/s is taken into account. In order to transform TOF distributions into mass distributions, the Jacobi factor dt/dm must be considered. Thus the measured TOF distributions are converted according to the formula

$$I(m)=\frac{I(t)\Delta t}{\Delta m}, \tag{1}$$

with $I(t)$ and $I(m)$ being the intensities in the TOF and mass spectra, respectively, and Δt and Δm being the corresponding channel widths in the time and mass domains. Δm is determined numerically for each channel of the TOF spectrum, taking into account the proper correlation between the time of flight and mass. Size distributions (in terms of the number N of atoms) are proportional to the mass distributions since $dm/dN=$ const.

C. Optical characterization of deposited films

Thin films grown from size-selected clusters have been investigated by photoluminescence and resonant Raman spectroscopy. To perform Raman spectroscopy on two films of size-selected clusters, samples V and VIII have been deposited on LiF since this substrate does not exhibit Raman peaks in the frequency range of interest. The spectra were obtained using an UV-specified Raman spectrometer (Dilor) equipped with a silicon photodiode array detector. The excitation wavelength was the 363.8-nm line (3.34 eV) of an argon-ion laser and the power was fixed to 20 mW, resulting in a power of 5 mW on the sample. The light was focused to a spot of 500 μm diameter. The spectrometer has been cali-

brated using a monocrystalline silicon wafer as a reference. The energy of the exciting photons is very close to the first direct electronic transition in silicon ($\Gamma_{25}-\Gamma_{15}=3.37$ eV).[21] These resonant conditions allow the detection of a Raman signal, even if the films are very thin.

The PL of the films has been measured using a Dilor *XY* Raman spectrometer in a special configuration. Instead of the classical foremonochromator, the diffused light passes through a notch filter cutting the laser excitation wavelength before it is dispersed by a 150-groves/mm grating. This configuration allows the acquisition of a large frequency window in one scan. PL spectra were taken using the 488-nm line (2.54 eV) of an argon-ion laser as well as the 647.1-nm line (1.92 eV) of a krypton-ion laser. All experiments have been performed at room temperature in the macroconfiguration (50-mm-focal-length objective) with the laser power on the sample kept at 250 μW. A liquid-nitrogen-cooled charge coupled device (CCD) chip has been used to detect the luminescence.

III. RESULTS

A. Size distribution of deposited clusters

Thin films of silicon clusters have been produced by selecting eight different parts of the total cluster pulse and depositing them on CaF_2 and LiF substrates. They are referred to as samples I–VIII. In order to determine the size distribution of the deposited particles, we have recorded mass spectra of the cluster pulse transmitted by the chopper. Since an accurate determination of the size distributions is very important for further analysis, we would like to explain the procedure in more detail for the case of sample II. The delay between the firing of the CO_2 laser and the opening of the chopper has been adjusted to $\Delta t_1=135$ μs, allowing clusters in the size range of 1000 atoms to pass through the chopper. Mass spectra of the transmitted cluster pulse have been recorded by probing the clusters arriving at the ionization region in steps of 5 μs. This is done by simply varying the delay Δt_2 between chopper opening and the firing of the ionizing excimer laser. The spectra are shown in Fig. 2. Only the six spectra recorded with 190 $\mu s \leqslant \Delta t_2 \leqslant 215 \mu$s show significant intensity caused by the transmitted silicon nanoparticles.

Besides small signals at ion flight times below 50 μs, which are caused from the residual background gas and pumping oil molecules, the TOF spectra show two distributions of detected ions, which are clearly separated from each other. Careful investigations of the dependence of the mass spectra on the fluence of the ionizing laser have shown that the first maximum at smaller flight times must be attributed to doubly ionized silicon clusters, while the second larger maximum belongs to singly ionized clusters. Furthermore, these studies revealed that the position of the second maximum practically did not change with the fluence of the ionizing laser, indicating that fragmentation and evaporation processes are negligible. Hence the distribution of the singly ionized clusters is considered to be a good approximation of the mass distribution of the neutral clusters in the beam. Moreover, it is seen from Fig. 2 that the position of the maximum shifts towards longer flight times when Δt_2 is increased. This reflects the fact that the particle pulse that has

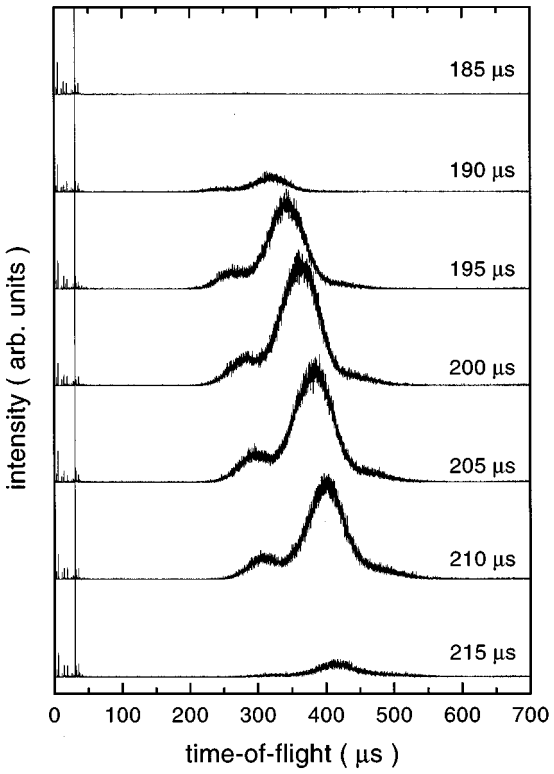

FIG. 2. Time-of-flight spectra of the silicon cluster pulse deposited on sample II. The delays Δt_2 between chopper opening and firing of the ionization laser are given in the figure.

passed through the chopper is broadened due to the size-dependent velocity of the clusters. Small (and fast) clusters reach the ionization region somewhat earlier than larger (and slower) particles.

The TOF spectra have been transformed to mass spectra as described in Sec. II B and two log-normal distributions have been fitted to the data, representing the doubly and singly ionized clusters, respectively. To obtain the total mass distribution of the deposited clusters, we have added all six log-normal curves representing the portion of singly ionized clusters in each mass spectrum. The result is shown in Fig. 3 as a dashed curve, while the single log-normal curves are

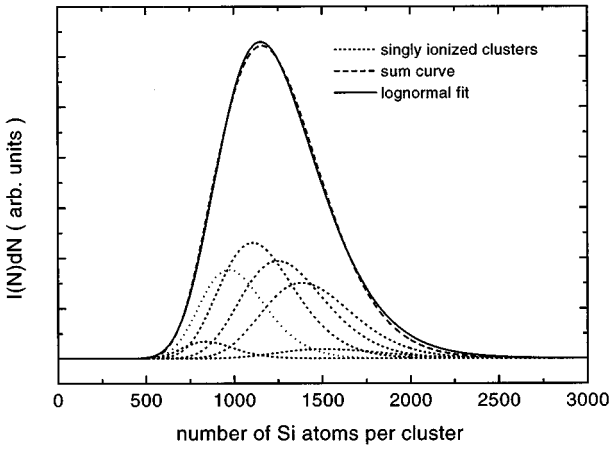

FIG. 3. Size distribution of silicon gas phase clusters deposited on sample II. The dotted lines are log-normal distributions fitted to the singly ionized cluster curves in the mass spectra of Fig. 2.

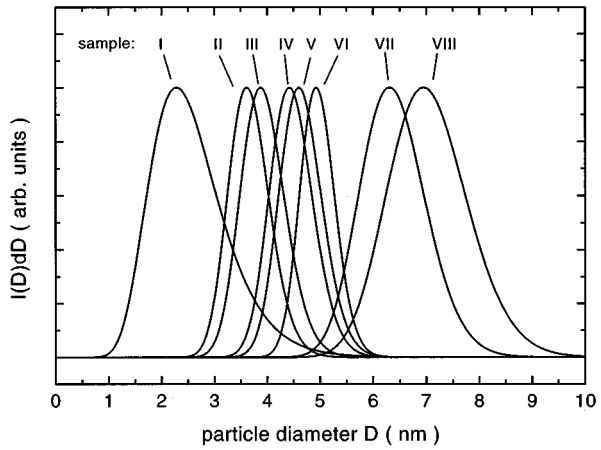

FIG. 4. Size distributions of the deposited clusters on samples I–VIII.

plotted as dotted lines. In order to obtain a quantitative description of the resulting distribution, again a log-normal function is fitted to the sum curve (solid curve in Fig. 3). This is considered to be the best representation of the mass distribution of the silicon particle pulse transmitted by the chopper.

To determine the size of the particles, the mass distribution $I(N)$ is transformed into a diameter distribution $I(D)$ using the relation

$$I(D)=I(N)\frac{dN}{dD}, \tag{2}$$

with

$$D(N)=\left(\frac{3N}{4\pi}V\right)^{1/3}. \tag{3}$$

$V=0.1601\ \mathrm{nm}^3$ is the volume of a unity cell in bulk silicon. Silicon clusters with eight different size distributions have been preselected and deposited on substrates (samples I–VIII). All size distributions are collected in Fig. 4 and their characteristic data are summarized in Table I. The experiments described in this article cover the range of mean diameters from $\overline{D}=2.5$ nm to $\overline{D}=7$ nm. The typical full width at half maximum is between 1 and 1.5 nm.

TABLE I. Size distributions of the deposited clusters.

Sample	$\overline{N}$	$\overline{D}$ (nm)	σ	E_{lum} (eV)
I	395	2.47	0.28	
II	1220	3.65	0.11	1.76
III	1575	3.92	0.11	1.68
IV	2310	4.46	0.09	1.68
V (LiF)	2600	4.63	0.09	1.58
VI	3175	4.95	0.07	1.49
VII	6755	6.37	0.10	
VIII (LiF)	9070	7.03	0.11	1.4 (weak)

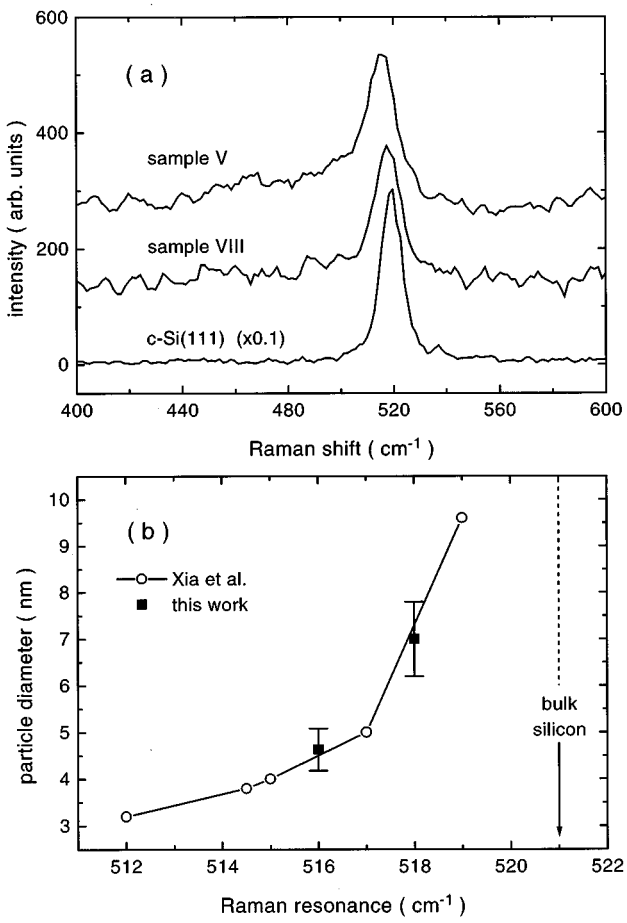

FIG. 5. (a) Raman spectra of samples V and VIII deposited on LiF, in comparison with a spectrum taken from c-Si(111). (b) Comparison of our results with the data published by Xia *et al.* (Ref. 22) (see the text for details).

B. Raman spectra of thin films

To verify that the covalent clusters, which have been deposited at low energy, do not fragment or coalesce, we have recorded Raman spectra of samples V and VIII. They are displayed in the upper part of Fig. 5 together with a Raman spectrum of c-Si(111). The spectra are characterized by a strong resonance around 520 cm^{-1}, caused by the Raman-allowed transition in crystalline silicon. A closer look reveals a shift of the resonance and a broadening of the peaks with decreasing particle size. The maximum of the spectrum taken from c-Si(111) is found at 520 cm^{-1}, whereas the maxima of the spectra taken from the nanocrystalline films are located at 516 and 518 cm^{-1} for samples V and VIII, respectively.

If the excitation is made with nonresonant light of longer wavelength (514.5 nm), the Raman peak of bulk silicon is located at 521 cm^{-1}. The redshift of 1 cm^{-1} in the present experiment is explained by a confinement effect due to the reduced penetration depth of the resonant 363.8-nm radiation. In contrast to the bulk, the nanocrystalline films are not affected by this process since the crystal sizes are smaller than the penetration depth, which is approximately 10–20 nm. So we determine a redshift of the resonance with respect to bulk silicon of 5 and 3 cm^{-1} for samples V and VIII, respectively.

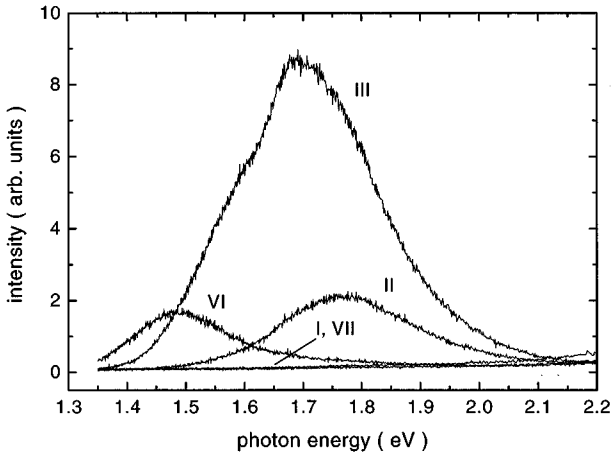

FIG. 6. Photoluminescence spectra of thin films, produced by size-selective deposition of silicon nanocrystals. The 488-nm line of an argon-ion laser was used for excitation.

Since the resonant excitation enhances the signal from the crystalline particle core relative to that from the surface region, the line shapes cannot be directly compared to the results of other experiments where the 514.5-nm line was used for excitation. But recently Xia *et al.*[22] have shown that the Raman spectrum of nanoscaled silicon, produced by PECVD of silane, can be decomposed into signals from the amorphous part and into surface and core contributions. From the shift of the nanocore contribution with respect to the bulk signal, they have calculated the diameters of the crystallites employing the strong phonon confinement model.[23,24] Their results were confirmed by x-ray studies, which yielded diameters in good agreement with those calculated from the Raman measurements. In the lower part of Fig. 5, we compare our results with those of Xia *et al.*[22] The error bars represent the full widths at half maximum of the corresponding size distributions (see Fig. 4). The agreement between the two data sets is very good. Moreover, our results are in good agreement with theoretical predictions for Si spheres presented by Campbell and Fauchet.[24]

In addition to the experiments with resonant excitation, we have performed Raman spectroscopy using visible excitation. These measurements have shown that there is also a small amount of amorphous silicon present in the samples.

In good agreement with other experiments employing low-energy cluster beam deposition,[18,19] we have found that the size of the free clusters is retained in the deposited cluster films. This proves the usefulness of mass spectrometry of gas phase nanoparticles for characterizing the thin films. The technique presented here should be even more powerful than the commonly used methods such as Raman spectroscopy, x-ray scattering, and electron microscopy since it gives immediate and unambiguous access to the size dispersion as well.

C. Luminescence spectra of thin films

In Fig. 6 the photoluminescence spectra are shown, which have been obtained using the 488-nm line of the argon-ion laser for excitation. The first interesting result is that no luminescence could be detected for the smallest and largest mean cluster sizes, though in the last case a very weak signal could sometimes be observed at photon energies around 1.4 eV. In contrast, strong luminescence signals were detected for the intermediate cluster sizes. It is seen in Fig. 6 that the maximum of the PL curves shifts from 1.5 to 1.75 eV when the particle size is varied from 5 nm to 3.6 nm. The spectra obtained by using the 647-nm line of a krypton-ion laser show qualitatively the same behavior, but are slightly higher in intensity, which is explained by the near-resonance excitation. After storing the samples in ambient air for several weeks, they have been checked again. No significant changes have been noticed. Samples that have not shown any PL before did not luminesce now and the maximum positions of the recorded spectra neither shifted nor showed significant changes in intensity.

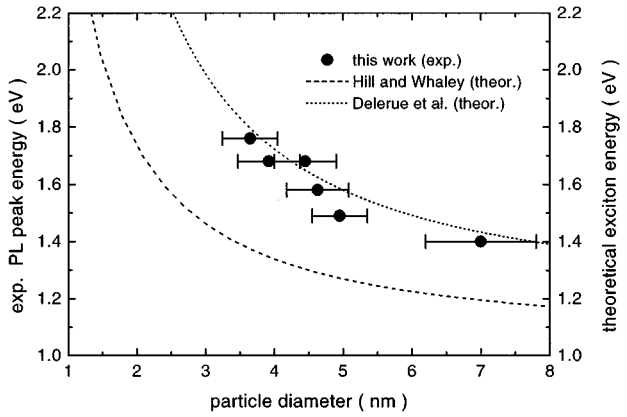

FIG. 7. Comparison of our data with recently published theoretical results from Delerue *et al.* (Ref. 5) and Hill and Whaley (Ref. 7).

In Fig. 7 we compare our results with recently published theoretical data for silicon nanocrystals saturated with hydrogen.[5,7] The calculations of Delerue *et al.*[5] have been carried out for particles up to 4.3 nm in diameter. A $d^{-1.39}$ law has been used to extrapolate the curve to larger particle diameters.[5] Our experimental findings are in good agreement with these theoretical results, while the curve predicted by Hill and Whaley[7] is shifted to smaller particle diameters or lower luminescence energies, respectively. The error bars indicate the full widths at half maximum of the size distributions shown in Fig. 4.

IV. DISCUSSION

Silicon nanoclusters have been generated by pulsed laser pyrolysis of SiH_4 in a gas flow reactor. The extracted clusters have been transferred to free molecular flow and analyzed by time-of-flight mass spectrometry. Thin films consisting of silicon nanoparticles with different narrow size distributions have been produced by size-selective deposition of the clusters at low energy. Resonant Raman spectra taken from the samples show that the films consist mainly of nanocrystalline silicon. The sizes of the crystals obtained by employing the generally accepted strong phonon confinement model[23,24] are in good agreement with the particle sizes determined by mass spectrometry. This proves that the particles do not fragment or coalesce after deposition. Hence our films consist of separated particles staggered onto each other.

The luminescence spectra recorded after exciting the films

with 488-nm and 647-nm radiation have shown the general trend that the luminescence peak shifts to higher energies as the particle diameter is decreased. The same trend has been observed for porous silicon produced by anodical etching of silicon wafers[9] or for oxidized nanocrystals produced by pyrolysis of disilane and oxidation at 700 °C–1000 °C.[12] However, our particles do luminesce at considerably shorter wavelength. Two different mechanisms have to be considered if our findings are compared with the results of Lockwood and Wang[9] and Schuppler *et al.*[12] They are related to (i) the shape of the particles and (ii) the surface passivation. It is known that silicon nanostructures produced by anodical etching form more wirelike structures. Theoretical calculations[5] of the luminescence of nanowires predict peak energies shifted to smaller values compared to spherical dots, depending on the orientation of the crystal lattice. This explains the differences between our results and those of Lockwood and Wang.[9]

The particles investigated by Schuppler *et al.*[12] have been produced by pyrolysis of disilane, which is similar to our technique, since both experiments start from gas phase precursors. But their particles have been oxidized in an O_2 atmosphere at 700 °C–1000 °C, while our particles are investigated as deposited. The contact to ambient air has been limited to a minimum by keeping the samples in an argon atmosphere before taking the first luminescence spectra. Since the spectra did not change after aging of the films in ambient air, we believe that oxidation plays a minor role in our experiments. This is supported by the fact that the smallest and largest clusters do not show luminescence, even if the samples are kept in air for weeks. Another argument against oxidation is the good agreement of the particle diameters determined from the Raman spectra with those derived from the mass spectrometry. If oxidation played a significant role one would expect larger Raman shifts since the crystalline core becomes smaller. Thus we believe that our films show the optical response of spherical silicon dots without a larger amount of oxidation. This assumption is also supported by the good agreement with the tight-binding results of Delerue *et al.*[5] This calculation was made with a higher-quality empirical parametrization for bulk Si than that used by Hill and Whaley, which accounts for the difference between the two theoretical curves.[25,26]

Although our results agree well with the quantum confinement theory, there is a problem with the film grown from the smallest clusters with a mean diameter of 2.5 nm. Considering the theoretical and experimental work known so far, we would expect luminescence around 2.2 eV. Therefore, the absence of any luminescence should not be attributed to insufficient energy of the exciting light. However, when the sample was irradiated with the UV laser (3.34 eV) used for taking the resonant Raman spectra a red-orange luminescence was clearly observed by the naked eye. Thus we are sure that the transition in the small clusters is above 2.54 eV. A possible explanation for this observation could be the reduction of the effective diameter of the particles due to oxidation. In this context, it should be noted that even one oxidic layer considerably reduces the diameter of the residual crystalline core. In addition, small variations in diameter will cause large changes in the band gap. Both effects are less critical if larger particles are concerned. Further experiments are in progress to measure the PL after UV excitation for all samples.

It is generally reported that there is a large Stokes shift of the PL energy compared to the band gap for small particles having diameters of about 2 nm or less. Many explanations have been given to rationalize the large Stokes shift, but all calculations actually use macroscopic models, assuming that the bulk structure is kept, even in small clusters containing a few hundreds or tenths of atoms. On the other hand, *ab initio* calculations[27] yield endohedrally self-doped fullerene structures for particles in the range of 1 nm. Moreover, a detailed knowledge of the phase transition to the diamond structure encountered in larger nanoparticles is still missing. Further experimental and theoretical work is clearly needed to investigate the properties of silicon particles with diameters smaller than 3 nm.

V. SUMMARY

We have shown that silicon films fabricated by deposition of size-selected neutral silicon clusters at low energy exhibit luminescence properties that are in remarkably good agreement with theoretical predictions based on the phonon confinement model. Our samples luminesce at higher peak energies than the particles with comparable diameters investigated in other experimental studies. This is mainly true for the medium-sized particles between 3.5 and 5 nm in diameter. Larger ones show very few luminescence, indicating an upper limit for the size of luminescent particles around 6 nm. For smaller particles the photon energy of the exciting radiation has to be increased. The main difference between our samples and others is that our particles are formed in the gas phase under high-purity conditions without wall interaction. Furthermore, no chemical or thermal treatment is used, which could induce strain in the particles or lead to wirelike structures. The good agreement with the calculations of Delerue *et al.*[5] leads to the conclusion that our films consist of zero-dimensional quantum dots without larger amount of oxidation.

ACKNOWLEDGMENTS

The authors would like to thank Professor H. Pauly for his continued interest and support. Fruitful discussions with Professor K. B. Whaley are gratefully acknowledged. This work was supported by the Deutsche Forschungsgemeinschaft in the frame of its Schwerpunktprogramm *Fine Solid Particles*.

[1] L. T. Canham, Appl. Phys. Lett. **57**, 1046 (1990).

[2] Y. Kanemitsu, Phys. Rep. **163**, 1 (1995).

[3] Ö. Dag, A. Kuperman, and A. Ozin, Adv. Mater. **7**, 72 (1995).

[4] E. C. Honea, A. Ogura, C. A. Murray, K. Raghavachari, W. O. Sprenger, M. F. Jarrold, and W. L. Brown, Nature (London) **366**, 42 (1993).

[5] C. Delerue, G. Allan, and M. Lannoo, Phys. Rev. B **48**, 11 024 (1993).

[6] L. W. Wang and A. Zunger, J. Phys. Chem. **98**, 2158 (1994).
[7] N. A. Hill and K. B. Whaley, Phys. Rev. Lett. **75**, 1130 (1995).
[8] F. Koch, V. Petrova-Koch, and T. Muschik, J. Lumin. **57**, 271 (1993).
[9] D. J. Lockwood and A. G. Wang, Solid State Commun. **94**, 905 (1995).
[10] S. Guha, P. Steiner, F. Kozlowski, and W. Lang, Thin Solid Films **276**, 73 (1996).
[11] J. Costa, P. Roura, A. Cannillas, E. Pascual, J. R. Morante, and E. Bertran, Thin Solid Films **276**, 96 (1996).
[12] S. Schuppler, S. L. Friedman, M. A. Markus, D. L. Adler, Y. H. Xie, F. M. Ross, Y. J. Chabal, T. D. Harris, L. E. Brus, W. L. Brown, E. E. Chaban, P. F. Szajowski, S. B. Christman, and P. H. Citrin, Phys. Rev. B **52**, 4910 (1995).
[13] M. Ehbrecht, M. Färber, F. Rohmand, V. V. Smirnov, O. M. Stelmakh, and F. Huisken, Chem. Phys. Lett. **214**, 34 (1993).
[14] M. Ehbrecht, H. Ferkel, V. V. Smirnov, O. M. Stelmakh, W. Zhang, and F. Huisken, Rev. Sci. Instrum. **66**, 3833 (1995).
[15] M. Ehbrecht, H. Ferkel, F. Huisken, L. Holz, Yu. N. Polivanov, V. V. Smirnov, O. M. Stelmakh, and R. Schmidt, J. Appl. Phys. **78**, 5302 (1995).
[16] M. Ehbrecht, H. Ferkel, V. V. Smirnov, O. M. Stelmakh, W. Zhang, and F. Huisken, Surf. Rev. Lett. **3**, 807 (1996).
[17] M. Ehbrecht, H. Ferkel, and F. Huisken, Z. Phys. D **40**, 88 (1997).
[18] V. Paillard, P. Melinon, V. Dupuis, J. P. Perez, A. Perez, and B. Champagnon, Phys. Rev. Lett. **71**, 4170 (1993).
[19] P. Melinon, V. Paillard, V. Dupuis, A. Perez, P. Jensen, A. Hoareau, J. P. Perez, J. Tuaillon, M. Broyer, J. L. Vialle, M. Pellarin, B. Baguenard, and J. Lerme, Int. J. Mod. Phys. B **9**, 339 (1995).
[20] W. C. Wiley and I. H. McLaren, Rev. Sci. Instrum. **26**, 1150 (1955).
[21] J. B. Renucci, R. N. Tyte, and M. Cardona, Phys. Rev. B **11**, 3885 (1975).
[22] H. Xia, Y. L. He, L. C. Wang, W. Zhang, X. N. Liu, X. K. Zhang, D. Feng, and H. E. Jackson, J. Appl. Phys. **78**, 6705 (1995).
[23] H. Richter, Z. P. Wang, and L. Ley, Solid State Commun. **39**, 625 (1981).
[24] I. H. Campbell and P. M. Fauchet, Solid State Commun. **58**, 739 (1986).
[25] C. Delerue, M. Lannoo, and G. Allan, Phys. Rev. Lett. **76**, 3038 (1996).
[26] N. A. Hill and K. B. Whaley, Phys. Rev. Lett. **76**, 3039 (1996).
[27] U. Röthlisberger, W. Andreoni, and M. Parrinello, Phys. Rev. Lett. **72**, 665 (1994).